Magnetoelectrodynamics of a three-dimensional organic conductor: Observation of cyclotron resonance in d_2[1,1;0]-(DMe-DCNQI)$_2$Cu

S. Hill and P. S. Sandhu
National High Magnetic Field Laboratory, 1800 E. Paul Dirac Drive, Tallahassee, Florida 32310

M. E. J. Boonman, J. A. A. J. Perenboom, and A. Wittlin
Research Institute for Materials and High Field Magnet Laboratory, University of Nijmegen, Toernooiveld 1, 6525 ED, Nijmegen, The Netherlands

S. Uji
National Research Institute for Metals, Tsukuba, Ibaraki 305, Japan

J. S. Brooks
National High Magnetic Field Laboratory, 1800 E. Paul Dirac Drive, Tallahassee, Florida 32310

R. Kato, H. Sawa, and S. Aonuma
Institute for Solid State Physics, University of Tokyo, Roppongi, Minato-ku, Tokyo 106, Japan
(Received 13 June 1996)

We have used an amplitude- and phase-sensitive millimeter-wave technique, in combination with a resonant cavity configuration, to observe cyclotron resonance in the three-dimensional organic conductor d_2[1,1;0]-(DMe-DCNQI)$_2$Cu. The data obtained in this way are simple to analyze and serve as an extremely clear illustration of the electrodynamic response of an organic conductor in a high magnetic field. A cyclotron resonance mass of $(3.35\pm0.2)m_e$ is obtained, in agreement with the effective mass deduced from de Haas–van Alphen measurements. This result suggests that Coulomb correlations between the three-dimensional charge carriers in this material are not important and that the large effective mass is simply a result of the hybridization between a narrow Cu $3d$ band and the $p\pi$ band due to the DMe-DCNQI molecules. [S0163-1829(96)01944-3]

I. INTRODUCTION

Over the past decade, organic conductors have attracted considerable interest due, in part, to their unique physical properties and also because of the versatility of these systems for the study of band formation.[1–5] Until recently, much of the activity has centered on the low-dimensional charge-transfer salts based on the organic donor molecules[2,4] tetramethyltetraselena-fulvalene (Refs. 1, 2, and 4) and BEDT-TTF [bis(ethylenedithio) tetrathia-fulvalene].[1,3,4] Although there have been many developments in the synthesis of these materials, their electronic structures remain low dimensional. In this work, we look at a molecular conductor that shows truly three-dimensional (3D) behavior.

Recently, an organic conductor containing Cu ions (DMe-DCNQI)$_2$Cu (DMe-DCNQI denotes 2,5-dimethyl-N,N′-dicyanoquinone-diimine) has been synthesized.[6] The planar DCNQI molecules are stacked in one-dimensional columns along the tetragonal c axis and are interconnected by tetrahedrally coordinated Cu ions.[7,8] A 1D Fermi surface is formed by the overlapping $p\pi$ orbitals of the stacked DCNQI molecules. The Cu ions, meanwhile, which form a sevenfold diamondlike lattice, are found to be in a mixed valence state[9] between Cu^+ and Cu^{2+}, indicating that the Cu $3d$ level lies close to the Fermi energy. Consequently, a 3D energy band is expected in addition to the 1D $p\pi$ energy band.[7,9] Recent de Haas–van Alphen (dHvA) studies by Uji *et al.*[10,11] have confirmed the existence of a 3D Fermi surface, in agreement with band-structure calculations.[7,12,13]

Various studies of deuterated and undeuterated alloys, $(DMe_{1-x}MeBr_x\text{-}DCNQI)_2Cu$, reveal a complex low-temperature phase diagram,[9–11,14–16] as shown in Fig. 1. In particular, the partially deuterated d_2[1,1;0]-(DMe-DCNQI)$_2$Cu compound shows reentrant metal-insulator-metal (M-I-M) phases.[16] The I phase is believed to

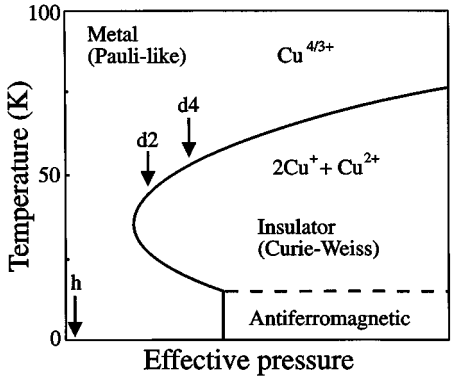

FIG. 1. Schematic of the experimentally determined temperature-pressure phase diagram for (DMe-DCNQI)$_2$Cu (Refs. 9–11 and 14–16); arrows indicate the positions of the deuterated salts ($d2$ and $d4$) with respect to the undeuterated (h) salt.

arise from a static ordering of the Cu ions ($\ldots Cu^{+}Cu^{+}Cu^{2+}\ldots$). A steep enhancement of the electronic specific-heat coefficient (γ) close to the insulating phase has been interpreted by some groups as evidence that Coulomb interactions drive the M-I and I-M transitions.[15] However, other groups fail to observe this enhancement of γ (Ref. 17) and, so, the issue as to whether Coulomb interactions are significant is still controversial.

dHvA measurements in the metallic phase for both deuterated and undeuterated (DMe-DCNQI)$_2$Cu single crystals yield rather large effective-mass values ($m^{*}>3m_e$).[10,11] These results could be interpreted as a further indication that Coulomb interactions lead to an enhancement of γ (proportional to the effective mass). However, band-structure calculations do indeed predict such large effective masses due to the hybridization between a narrow Cu $3d$ band and the $p\pi$ band due to the DMe-DCNQI molecules;[7,12,13] i.e., this picture is consistent with the mixed valence character of the Cu ions in the metallic phase. Furthermore, similar effective masses are found for both deuterated and undeuterated samples;[10,11] i.e., γ shows no enhancement on approaching the M-I phase boundary.

The present study is motivated by several factors: First, any renormalization of the quasiparticle effective mass, due to Coulomb interactions, is expected to be energy and wave-vector dependent;[18] therefore, different measurements should yield different effective-mass values. In the language of strongly interacting fermions,[18] thermodynamic measurements yield the quasiparticle effective mass m^{*}, which includes contributions from band-structure, electron-phonon, and electron-electron interactions. In contrast, cyclotron resonance (CR), which couples to the center-of-mass motion of an electronic system,[19,20] probes the dynamical mass m_λ and is insensitive to Coulomb interaction effects.[18–20] Therefore, a comparison between thermodynamic (dHvA) and CR masses would be a natural way to settle the argument over the role of Coulomb correlations in the title compound. Such a comparison is particularly important in view of the fact that tight-binding band-structure calculations (as in Refs. 7, 12 and 13) only predict the ratios of effective masses corresponding to different Fermi surface sections; i.e., they do not produce absolute values.[21]

Second, recently there have been a number of reports of CR in some of the quasi-two-dimensional (2D) BEDT-TTF salts.[20,22–24] In each case, there is a difference between the effective masses deduced from CR and those determined from thermodynamic and/or magnetotransport measurements,[20,22–24] suggesting that Coulomb correlations may play an important role in the quasi-2D organic conductors. In view of this, it is interesting to compare these findings with measurements on a 3D organic conductor.

Finally, existing optical data on the organics have been difficult to interpret due to the rather weak features attributed to CR. Matters are further complicated by the highly anisotropic conduction in these metals; this is particularly so in the quasi-2D salts. An understanding of CR data in these materials relies heavily on a good knowledge of certain factors such as the conductivities and relaxation times, together with any anisotropy in these quantities. We will show that the data obtained by our experimental technique can be successfully modeled, giving rise to an accurate determination of the CR mass.

II. EXPERIMENTAL CONSIDERATIONS

A millimeter-wave vector network analyzer[25] (MVNA) was configured to monitor the reflected phase and amplitude of millimeter wave radiation coupled to a resonant cavity containing the samples. The MVNA allows measurements in a very extended frequency range (8–350 GHz); the measurements reported here were performed in the 70–130-GHz range ($\lambda\sim 2$–4 mm) where the MVNA has a dynamic reserve in excess of 90 dB. Partially deuterated d_2[1,1;0]-(DMe-DCNQI)$_2$Cu samples were chosen for this study because of their reentrant M-I-M behavior.[9–11,14–16]

The use of resonant cavities offers many advantages in this frequency regime, particularly in the case of small metallic crystals, where the radiation wavelength is comparable to the sample dimensions.[26,27] Under these conditions, the sample acts as a perturbation of the electromagnetic field distribution within the cavity.[26,27] Due to the resonant nature of the problem, the resonance condition is very sensitive to small changes in the sample conductivity. Another advantage of this technique is that, by carefully positioning the sample within the cavity, one can excite ac currents in any desired direction within the sample.[26] Furthermore, it is possible to selectively couple to either the electric or magnetic dipole fields within the cavity.[26]

The so-called ''cavity perturbation'' technique has been used by several groups to study organic conductors,[26,28–30] however, there are relatively few reports combining this technique with high magnetic fields.[24] Polisskii *et al.*[24] have observed CR in the quasi-two-dimensional α-(BEDT-TTF)$_2$NH$_4$Hg(NCS)$_4$ salt; a rectangular cavity is employed and the transmitted amplitude is monitored for a few frequencies between 50 and 105 GHz. In this work, we utilize the full vector capability (i.e., phase and amplitude) of the MVNA, enabling a precise understanding of the coupling between our conducting samples and the microwave fields in the cavity. Furthermore, we have developed a technique that allows measurements to be performed at many closely spaced frequencies over a fairly extended frequency range.

A detailed description of our experimental setup is reported elsewhere.[31] An oversized cylindrical copper cavity was employed (diameter 12.5 mm, height 20 mm), providing many resonant modes in the desired frequency range. Four small needlelike d_2[1,1;0]-(DMe-DCNQI)$_2$Cu samples (length $\sim$3 mm, width $\sim$200 μm) were inserted into a thin slice of styrofoam so that their c axes (needle axis) coincided. The measurements were then performed with the dc magnetic field applied parallel to these needles. By exciting transverse electric modes, we can assume that there is an electric field antinode at a distance $\lambda/4$ above the bottom of the cavity; this electric field acts in a plane perpendicular to the axis of the cavity. With this in mind, the styrofoam sample holder was placed close to the bottom of the cavity in such a way as to excite currents in the samples in a plane perpendicular to the applied dc magnetic field, i.e., in the ab plane.

An oversized cylindrical waveguide was used to pass radiation from the spectrometer, through our cryostat, and into

the bore of the magnet. Smooth conical transitions were inserted wherever changes in the waveguide diameter might lead to impedance mismatches, thereby minimizing unnecessary reflections. The radiation was then coupled to, and from, the cavity via a 1.4-mm ($\sim\lambda/4-\lambda/2$) aperture centered on the top of the cavity. Discrimination between the incident and reflected radiation was achieved by means of an optical beam splitter. The samples and the cavity were maintained at 1.2 K and placed at the maximum magnetic field position within a 20-T resistive magnet. Once cooled, the frequency sweeping capability of the MVNA could be used to identify resonant modes of the loaded cavity. All measurements were then performed at a fixed frequency, while sweeping the magnetic field. A quartz-locking frequency counter stabilized the source frequency to the cavity resonances.

III. ANALYSIS

In analyzing our data, we shall consider the surface impedance of the sample, $\mathbf{Z}_s=\mathbf{R}_s+i\mathbf{X}_s$, where $\mathbf{R}_s$ is the surface resistance and $\mathbf{X}_s$ is the surface reactance.[26] This is a common approach for good conductors in the so-called ''skin depth'' regime, where the skin depth is much smaller than the sample dimensions and, therefore, the ac electromagnetic fields are not uniform within the sample. The surface impedance is given by the expression

$$\mathbf{Z}_s=\left(\frac{i\mu_0\omega}{\sigma_1-i\sigma_2}\right)^{1/2}, \tag{1}$$

where $\sigma(=\sigma_1-i\sigma_2)$ is the complex conductivity, $\omega/2\pi$ the frequency, and μ_0 the free space permeability. Solving for R_s and X_s in terms of σ_1 and σ_2, we obtain

$$R_s=\Omega(1+\alpha)^{1/2}, \quad X_s=\Omega(1-\alpha)^{1/2}, \tag{2}$$

where

$$\Omega=\left[\frac{(\mu_0\omega)^2}{4(\sigma_1^2+\sigma_2^2)}\right]^{1/4}, \quad \alpha=\frac{\sigma_2}{(\sigma_1^2+\sigma_2^2)^{1/2}}.$$

To demonstrate that a good single crystal of $(DMe\text{-}DCNQI)_2Cu$ is in the skin-depth regime when microwave radiation is coupled to the sample in this geometry, we estimate the skin depth $[\delta=(\pi f\sigma_1\mu_0)^{-1/2}]$ to be about 1 μm, assuming a value of σ_1 of $3\times10^4\ \Omega^{-1}\,\mathrm{cm}^{-1}$ in the ab plane and at 1 K;[32] this is small when compared to the smallest sample dimension.

With the dc magnetic field applied parallel to the c axis, only a single dHvA oscillation is observed,[10,11] corresponding to a single closed orbit in k space; this is the α orbit. By exciting ac currents in the ab plane, it should, in principle, be possible to observe CR due to the α orbit. The complex conductivity will then be given by

$$\sigma=\frac{1}{2}\frac{ne^2\tau}{m_\alpha}\left[\frac{1+i(\omega-\omega_c)\tau}{1+(\omega-\omega_c)^2\tau^2}+\frac{1+i(\omega+\omega_c)\tau}{1+(\omega+\omega_c)^2\tau^2}\right], \tag{3}$$

where ω_c $(=e\mathbf{B}/m_\alpha)$ is the cyclotron frequency and τ is the relaxation time; m_α is the CR mass due to the α orbit, n is the carrier density, and $\mathbf{B}$ is the applied dc magnetic field. Both resonant (left-hand term in square brackets) and nonresonant (right-hand term in square brackets) contributions to the ac conductivity are considered in the above expression; this is due to the fact that the radiation everywhere in the cavity may be separated into left and right circularly polarized components. No special considerations are made about the exact shape of the Fermi surface; i.e., Eq. (3) is derived for a free electron gas.

Changes in the sample conductivity and, therefore, its surface impedance, result in the following changes in the cavity resonance parameters:[26]

$$\frac{\Delta\Gamma}{2f_0}=\tfrac{1}{2}\Delta(1/Q)=\xi\Delta R_s, \quad \frac{\Delta f}{f_0}=\xi\Delta X_s. \tag{4}$$

In the above expressions, $\Delta\Gamma$ is the change in the width of the resonance, Δf is the change in the resonance frequency f_0, Q is the quality factor, and ξ is a geometrical factor.[26] Therefore, on application of a dc magnetic field, we can relate changes in these quantities (Q, f_0, etc.) to changes in the surface impedance of the sample.

In our experiment, changes in the resonance frequency f_0 will result in changes in the phase of the radiation reflected from the cavity, while changes in the resonance quality factor (Q or Γ) will lead to changes in amplitude.[25,31] More precisely,

$$\Delta\phi\propto\frac{\Delta f}{f_0}\propto\Delta X_s, \quad \frac{1}{\Delta A}\propto\Delta\Gamma\propto\Delta R_s, \tag{5}$$

where ϕ and A are the reflected phase and amplitude, respectively. Here we see the virtue of the vector capability of the MVNA, which allows us to extract both components of the surface impedance with a single measurement.

IV. RESULTS

Figure 2 shows typical results for several frequencies between 83.87 and 125.24 GHz; the temperature is 1.2 K in each case. Also included in Fig. 2 are fits to the data according to the above analysis. In order to achieve good fits, a complex linear term was subtracted from the raw data, which we attribute to several external factors, e.g., magnetoresistance in the waveguide and variations in the coupling between the spectrometer and the cavity; the latter is a result of standing waves in the waveguide and mechanical changes in its length caused by thermal fluctuations. The reason for the apparent increase in noise as the frequency is increased is due to two factors: (i) the dynamic range of the MVNA decreases with increasing frequency, and (ii) the cavity becomes overcoupled at higher frequencies resulting in a reduction in the cavity Q factor. For these reasons, no scale is assigned to the vertical axes in Fig. 2 since the noisier curves have had to be expanded by up to a factor of 20 for the sake of clarity. Furthermore, the geometrical factor ξ appearing in Eq. (4) cannot be determined in this experiment; i.e., Fig. 2 displays qualitative changes in R_s and X_s.

From fits to the data, an average CR mass value of $m_\alpha=(3.37\pm0.2)m_e$ is obtained and, in every case, a scatter-

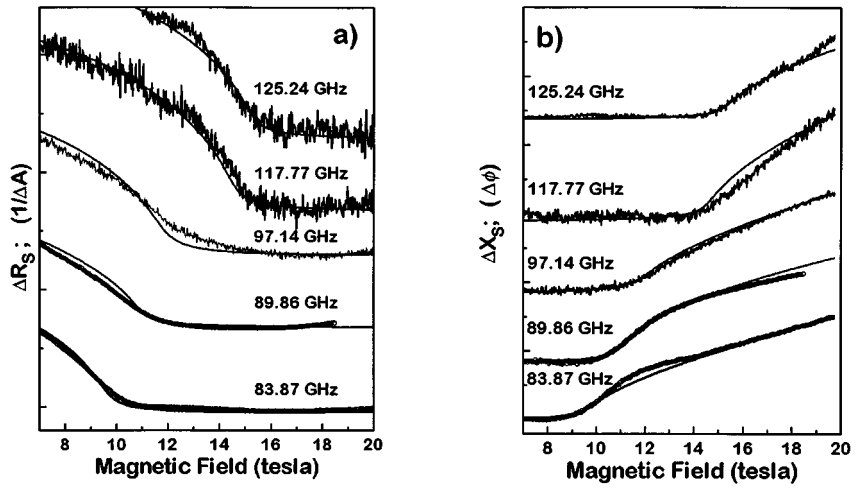

FIG. 2. (a) Change in the surface resistance ($\Delta R_s \propto 1/\Delta A$), and (b) the surface reactance ($\Delta X_s \propto \Delta\phi$), as a function of the applied dc magnetic field for several different frequencies; the temperature is 1.2 K in each case. The smooth curves through the data have been fitted according to the analysis described in the text. The higher-frequency data have been expanded for the sake of clarity.

ing rate of $\tau^{-1}=2\times10^{10}\ \mathrm{s}^{-1}$ gave the best results. Agreement between experiment and analysis is remarkably good over the entire field and frequency range. Similar results were obtained at many other frequencies in the range 70–130 GHz. By plotting the magnetic field value above which the phase begins to increase sharply (see Fig. 2), as a function of frequency, we obtain an independent estimate of the CR mass; such a plot, together with a linear fit, is shown in Fig. 3. Using this method, we obtain a value for the CR mass of $m_\alpha=(3.34\pm0.2)m_e$, which is fully consistent with the earlier estimate. What is more, to within experimental errors, these values of the CR mass agree with the effective mass deduced from dHvA studies,[10] i.e., $m_\alpha=(3.3-3.4)m_e$.[33]

V. DISCUSSION

The fact that exactly the same values for m_α are obtained from dHvA and CR measurements seems to rule out strong Coulomb correlations between carriers on the 3D Fermi surface in d_2[1,1;0]-(DMe-DCNQI)$_2$Cu. This result, coupled with the dHvA results, which indicate that m_α is the same for deuterated and undeuterated salts,[10,11] suggests that Coulomb correlations between the 3D carriers play no significant role in the entire (DMe-DCNQI)$_2$Cu family. Therefore, we conclude that the large m_α is simply a result of the hybridization between a narrow Cu 3d band and the $p\pi$ band due to the DMe-DCNQI molecules.

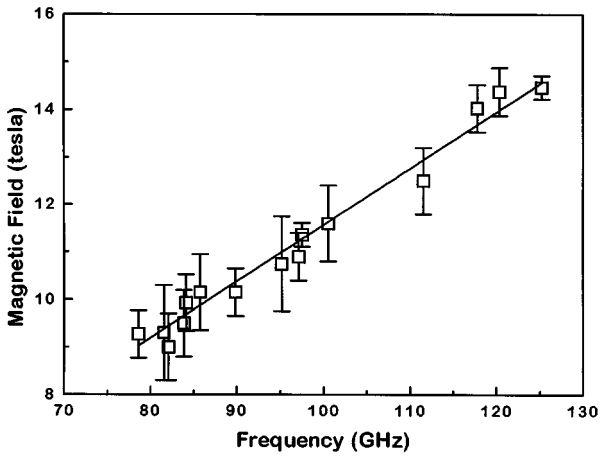

FIG. 3. A plot of the resonance field positions against frequency. The straight line fit may be used to make an accurate determination of the CR effective mass.

One then has to ask why correlations apparently play an important role in some of the quasi-2D organic conductors.[20,22–24] One possibility is that the reduced dimensionality of the quasi-2D systems leads to an enhancement of the Coulomb interactions. However, the BEDT-TTF and (DMe-DCNQI)$_2$Cu systems differ in many other respects[5] (i.e., not just dimensionality), so there may be many other explanations.

Since CR and dHvA measurements probe only the 3D Fermi surface, one cannot rule out the possibility that Coulomb correlations between carriers on the 1D Fermi surface are significant. One way to verify this would be to look for signatures in the surface impedance for quasi-1D CR. This possibility was first suggested by Gor'kov and Lebed'[34] and has been discussed elsewhere.[35,36] In order to do this, a different experimental configuration should be devised and further work in this direction is currently in progress.

The form of the amplitude and phase variation in Fig. 2 is not typical for CR; it is more usual to observe a Lorentzian resonance line shape as seen, e.g., in doped semiconductors. The reason for this is because, in the present case, we are dealing with a highly conducting sample in a resonant cavity and, under these conditions, it is the boundary condition between the sample surface and the surrounding vacuum that determines the cavity response [see Eqs. (2)–(5)]. This type of result has been observed previously in experiments on semimetallic bismuth involving a resonant microwave bridge technique.[37,38] In a semiconductor, however, electromagnetic radiation will penetrate the entire sample (quasistatic approximation) and, therefore, its bulk dielectric response ($\varepsilon=\varepsilon_1+i\varepsilon_2$) dictates the CR line shape; ε_1 and ε_2 are directly related to σ_2 and σ_1, respectively, thereby accounting for a Lorentzian line shape [see Eq. (3)].

Figure 4 shows the predicted field dependence of the phase and amplitude, in the ''skin depth'' regime, for several different values of $\omega\tau$. It is interesting to note the entirely different field dependence of R_s in the case of $\omega\tau>1$ and $\omega\tau<1$. In the limit $\omega\tau\ll1$, the well-known ''Hagen Rubens'' limit is reached when $\sigma_1\gg\sigma_2$ and $R_s\approx X_s$ [see Eq. (1)]. In

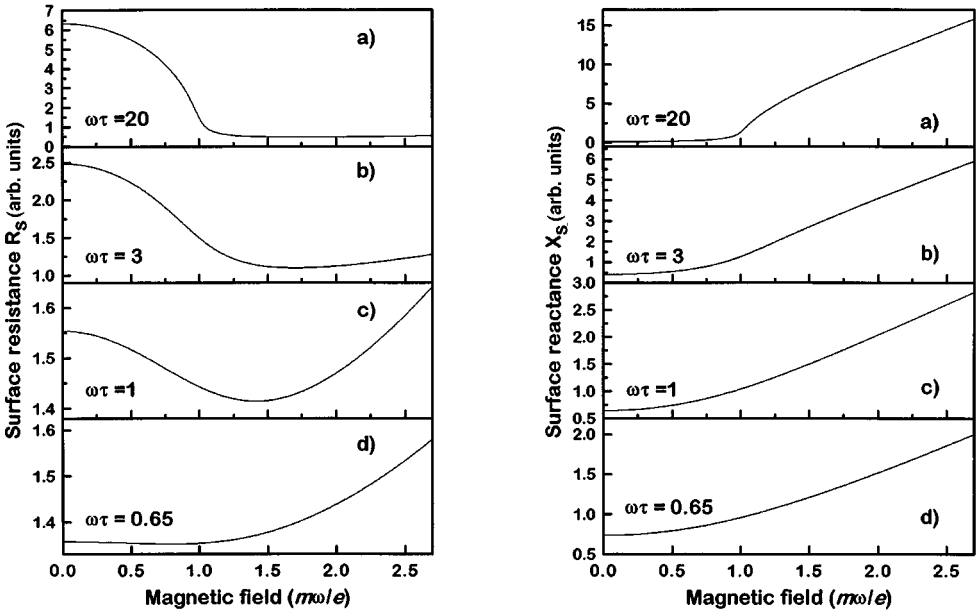

FIG. 4. Predicted field dependence [normalized to the cyclotron resonance field ($m\omega/e$)] of the surface resistance (R_s) and surface reactance (X_s) for different values of $\omega\tau$.

this limit, the transport properties of the sample are probed, which can be seen, to a certain extent, in Fig. 4(d) where R_s and X_s begin to resemble the magnetoresistance of a typical metal. By extending our measurements to lower frequencies, it should be possible to observe this crossover. For the data shown in Fig. 2, $\omega\tau\sim10$, therefore, it would be necessary to go below 10 GHz in order to check this. Alternatively, measurements on less pure samples (shorter τ) could access this regime.

In view of the above, we comment briefly here on some of the results obtained by Pollisskii *et al.*, for ac coupling to the highly conducting planes of the quasi-2D organic metal α-$(BEDT\text{-}TTF)_2NH_4Hg(NCS)_4$, with the magnetic field applied normal to these planes, i.e., a similar geometry to the experiments reported here. They plot absorption versus magnetic field for a frequency of 50.3 GHz: A broad peak is observed at low fields, corresponding to a CR mass $1.8m_e$, while at higher fields the absorption starts to increase sharply in identical fashion to the behavior of R_s shown in Fig. 4(b). The authors comment on this behavior, but make no assignment of this feature of their data. The broad peak seen at lower fields is also observed for ac coupling in the interplane (low conductivity) direction, when radiation will penetrate the entire sample; hence this fairly symmetric peak is attributed to CR. Due to anisotropy in the BEDT-TTF conductors, it is far easier to excite ac currents in the interplane direction than within the highly conducting planes.[39] Therefore, we suggest that the results in Ref. 24, for the in-plane geometry, include effects due to both intraplane and interplane currents. For the inplane currents, their data imply $\omega\tau<1$, while for the interplane currents, $\omega\tau$ must be greater than unity in order to observe CR. This raises the question as to whether τ is highly anisotropic in these materials, or whether these two features of the data are of a different origin. Furthermore, a comparison between their data and R_s in Fig. 4(d) indicates that a larger cyclotron mass may be appropriate, thus accounting for the apparent difference between CR and magnetotransport measurements.

VI. SUMMARY

We have observed CR in the 3D organic conductor d_2[1,1;0]-$(DMe\text{-}DCNQI)_2Cu$. We obtain a CR mass that is in agreement with the effective mass obtained from dHvA measurements. This rules out the possibility that correlations between the 3D carriers play an important role in these materials. Therefore, we suggest that the large effective mass is simply a result of the hybridization between a narrow Cu $3d$ band and the $p\pi$ band due to the DMe-DCNQI molecules.

In this work, we have studied, by far, the simplest geometry for the $(DMe\text{-}DCNQI)_2Cu$ system. We have been able to neglect the quasi-1D character associated with this material along its c axis.[7,12] Clearly, much work remains to be done in understanding the magnetoelectrodynamics of these, and other, highly anisotropic organic conductors. We also note that, in many of the organic conductors that are currently of interest, sample quality is such that typical scattering rates are comparable to the frequencies used in this study, i.e., $\omega\tau\sim1$. Therefore, this general experimental area offers great potential in understanding the electrodynamics of these materials in high magnetic fields. We conclude by emphasizing the power of the vector measurement technique in combination with a resonant cavity configuration. The data obtained in this way are simple to analyze and serve as an extremely clear illustration of the electrodynamics of an organic conductor in high magnetic fields.

ACKNOWLEDGMENTS

This work was supported by the National Science Foundation under Grant No. NSF-DMR 95-10427. The work in Nijmegen was part of the research program of the ''Stichting voor Fundamenteel Onderzoek der Materie,'' which is financially supported by the ''Nederlandse Organisatie voor Wetenschappelijk Onderzoek'' and has been supported by the European Commission under Contract No. CHGT-CT93-0051. The authors would also like to thank P. Goy of AB*mm* for his advice and expertise and Dr. A. Polisskii for useful discussion.

[1] T. Ishiguro and K. Yamaji, *Organic Superconductors*, Springer Series in Solid State Sciences Vol. 88 (Springer-Verlag, Berlin, 1990).

[2] S. Kagoshima, H. Nagasawa, and T. Sambongi, *One-Dimensional Conductors*, Springer Series in Solid State Sciences Vol. 72 (Springer-Verlag, Berlin, 1987).

[3] V. Kresin and W. Little, *Organic Superconductivity* (Plenum, New York, 1990).

[4] J. Wosnitza, *Fermi Surfaces of Low Dimensional Organic Metals and Superconductors*, Springer Tracts in Modern Physics Vol. 134 (Springer-Verlag, Berlin, 1996).

[5] For a review, see, e.g., Synth. Met. **71** (1995).

[6] A. Aumüller, P. Erk, G. Klebe, S. Hünig, J. U. von Schütz, and H.-P. Werner, Angew. Chem. Int. Ed. Engl. **25**, 740 (1986).

[7] R. Kato, H. Kobayashi, and A. Kobayashi, J. Am. Chem. Soc. **111**, 5224 (1989).

[8] K. Sinzger, S. Hünig, M. Jopp, D. Bauer, W. Bietsch, J. U. von Schütz, C. Wolf, R. K. Kremer, T. Metzenthin, R. Bau, S. I. Kahn, A. Lindbaum, C. L. Lengauer, and E. Tillmanns, J. Am. Chem. Soc. **115**, 7696 (1993).

[9] H. Kobayashi, A. Miyamoto, R. Kato, F. Sakai, A. Kobayashi, Y. Yamakita, Y. Furukawa, M. Tasumi, and T. Watanabe, Phys. Rev. B **47**, 3500 (1993).

[10] S. Uji, T. Terashima, H. Aoki, J. S. Brooks, R. Kato, H. Sawa, S. Aonuma, M. Tamura, and M. Kinoshita, Phys. Rev. B **50**, 15 597 (1994).

[11] S. Uji, T. Terashima, H. Aoki, J. S. Brooks, R. Kato, H. Sawa, S. Aonuma, M. Tamura, and M. Kinoshita, Solid State Commun. **93**, 203 (1995).

[12] A. Kobayashi, R. Kato, H. Kobayashi, T. Mori, and H. Inokuchi, Solid State Commun. **64**, 45 (1987).

[13] R. Kato, S. Aonuma, and H. Sawa, Synth. Met. **70**, 1071 (1995).

[14] R. Kato, H. Sawa, S. Aonuma, M. Tamura, M. Kinoshita, and H. Kobayashi, Solid State Commun. **85**, 831 (1993).

[15] Y. Nishio, K. Kajita, W. Sasaki, R. Kato, A. Kobayashi, and H. Kobayashi, Solid State Commun. **81**, 437 (1992).

[16] S. Aonuma, H. Sawa, R. Kato, and H. Kobayashi, Chem. Lett. 513, 1993.

[17] S. Kagoshima, Y. Saito, T. Hasegawa, N. Wada, H. Yano, R. Kato, N. Miura, and H. Kobayashi, Synth. Met. **70**, 1065 (1995).

[18] K. F. Quader, K. S. Bedell, and G. E. Brown, Phys. Rev. B **36**, 156 (1987).

[19] W. Kohn, Phys. Rev. **123**, 1242 (1961).

[20] J. Singleton, F. L. Pratt, M. Doporto, W. Hayes, T. J. B. M. Janssen, J. A. A. J. Perenboom, M. Kurmoo, and P. Day, Phys. Rev. Lett. **68**, 2500 (1992).

[21] C. E. Campos, P. S. Sandhu, J. S. Brooks, and T. Ziman, Phys. Rev. B **53**, 12 725 (1996).

[22] S. V. Demishev, A. V. Semeno, N. E. Sluchanko, N. A. Samarin, I. B. Voskoboinikov, V. V. Glushkov, J. Singleton, S. J. Blundell, S. O. Hill, W. Hayes, M. V. Kartsovnik, A. E. Kovalev, M. Kurmoo, P. Day, and N. D. Kushch, Phys. Rev. B **53**, 12 794 (1996).

[23] S. Hill, J. Singleton, F. L. Pratt, W. Hayes, T. J. B. M. Janssen, J. A. A. J. Perenboom, M. Kurmoo, and P. Day, Synth. Met. **55-57**, 2566 (1993).

[24] A. Polisskii, J. Singleton, P. Goy, W. Hayes, M. Kurmoo, and P. Day, J. Phys. C **8**, L195 (1996).

[25] P. Goy, M. Gross, and J. M. Raimond, in *Proceedings of the 15th International Conference in Infrared and Millimeter Waves, Orlando, 1990* edited by R. J. Temkin (Plenum, London, 1990), C. Dahl, P. Goy, and J-P. Kotthaus, in Millimeter-Wave Spectroscopy of Solids, edited by G. Grüner (Springer Verlag, Berlin, in press).

[26] O. Klein, S. Donovan, M. Dressel, and G. Grüner, Int. J. Infrared Millimeter Waves **14**, 2423 (1993); S. Donovan, O. Klein, M. Dressel, and G. Grüner, *ibid*. **14**, 2459 (1993); M. Dressel, O. Klein, S. Donovan, and G. Grüner, *ibid*. **14**, 2489 (1993).

[27] L. I. Buranov and I. F. Shchegolev, Instrum. Expt. Tech. **14**, 528 (1971).

[28] O. Klein, K. Holczer, G. Grüner, J. J. Chang, and F. Wudl, Phys. Rev. Lett. **66**, 655 (1991).

[29] M. Dressel, S. Bruder, G. Grüner, K. D. Carlson. H. H. Wang, and J. M. Williams, Phys. Rev. B **48**, 9906 (1993).

[30] J. L. Musfeldt, M. Poirer, P. Batail, and C. Lenoir, Phys. Rev. B **52**, 15 983 (1995) **51**, 8347 (1995).

[31] S. Hill, P. S. Sandhu, C. Buhler, S. Uji, J. S. Brooks, L. Seger, M. Boonman, A. Wittlin, J. A. A. J. Perenboom, P. Goy, R. Kato, H. Sawa, and S. Aonuma (unpublished).

[32] R. Kato (private communication).

[33] A dHvA measurement of m_α is only available for the undeuterated and fully deuterated salts. However, to within experimental error ($\approx$10%), all other dHvA effective masses are the same for all these salts (see Refs. 10 and 11).

[34] L. P. Gor'kov and A. G. Lebed', Phys. Rev. Lett. **71**, 3874 (1993).

[35] S. Hill, Ph.D. thesis, University of Oxford, 1994.

[36] A. Ardavan, J. Singleton, W. Hayes, A. Polisskii, P. Goy, M. Kurmoo, and P. Day, Synth. Met. (to be published).

[37] J. K. Galt, W. A. Yager, F. R. Merritt, B. B. Cetlin, and A. D. Brailsford, Phys. Rev. **114**, 1396 (1959).

[38] J. K. Galt, W. A. Yager, F. R. Merritt, B. B. Cetlin, and H. W. Dail, Phys. Rev. **100**, 748 (1955).

[39] S. Hill *et al.*, Phys. Rev. B (to be published).